Environment Protection Engineering

Vol. 47 2021 No. 3

DOI:10.37190/epe210304

BRUNO KOSTURA (ORCID 0000-0002-8019-4524)[1]
RADIM HUCZALA (ORCID 0000-0002-6464-9986)[1]
ZDENĚK KLIKA (ORCID 0000-0002-5261-3648)[1]
MICHAL RITZ (ORCID 0000-0002-1679-3055)[1]
LUCIE BARTOŇOVÁ (ORCID 0000-0003-3387-4057)[1]
DALIBOR MATÝSEK (ORCID 0000-0002-1412-1079)[2]

UPTAKE OF PHOSPHATES FROM WATER SOLUTIONS ON METALLURGICAL SLUDGE

Steel-making dust slurry (SS) and convertor dust slurry (CS) were tested for uptake of phosphates from aqueous solutions. The adsorption of phosphates on SS and CS corresponded well with both Langmuir and Freundlich adsorption isotherms, which indicated the combination of physical and chemical processes. The maximum adsorbed amount of phosphates on both dust slurry samples was ca. 11 mg P/g. The study evaluates also the effect of acidic leaching on the retention characteristics of both dust slurry samples. From the slurry samples prepared by acidic leaching, the leached convertor dust slurry (CSL) was the only sample capable to retain phosphates. To reveal the retention mechanisms of phosphates, the original and leached dust slurry samples were analyzed by IR and Raman spectroscopy. Co-precipitation of Ca and Fe phosphates, or surface complexation of phosphates were evaluated as the retention mechanisms of CS and CSL while the retention of phosphates by zincite in the case of SS is probably based on their adsorption.

1. INTRODUCTION

One of the most problematic wastes originating from the metallurgy of iron are fine-grained metallurgical wastes coming from wet cleaning of waste gases. These materials contain not only high iron levels but also high concentrations of heavy metals, namely Zn, Cd, and Pb. Therefore, as being considered as hazardous waste materials, their disposal represents an environmental hazard. These materials can be partially processed by pyrometallurgical [1] or hydrometallurgical methods [2]. The purpose of these two

[1]Department of Chemistry, VSB – Technical University of Ostrava, 17. listopadu 15/2172, 708 33 Ostrava, Czech Republic, corresponding author B. Kostura, email address: bruno.kostura@vsb.cz

[2]Institute of Geological Engineering, VŠB – Technical University of Ostrava, 17. listopadu 15/2172, 708 33 Ostrava, Czech Republic.

methods is the separation of heavy metals, namely Zn. Then, the processed dust slurry is partially reused in metallurgical processes and the rest is disposed. One of the possibilities how to prevent landfilling is the utilization of processed dust slurry as an adsorbent. For this reason, these materials are frequently studied as adsorbents for the retention of heavy metals.

For example, in the study described by Loậ Pez-Delgado et al. [3], the adsorption of Pb^{2+}, Zn^{2+}, Cd^{2+}, Cu^{2+} and Cr^{3+} from aqueous solutions on steel-making dust slurry was studied. Blast-furnace dust slurry was studied as an adsorbent for the retention of Ni^{2+} from aqueous solutions [4] and utilization of convertor dust slurry for the adsorption of Mn, Co, and Ni from mine wastewater was evaluated by Rozumová et al. [5]. Abundant studies are dealing with the retention of metal cations on other adsorbents than metallurgical dust slurry samples, e.g., on clay minerals, and its dominant mechanism is usually adsorption or ionic exchange [6].

Studies related to the testing of metallurgical wastes for the retention of anions are quite scarce. For example, the adsorption of arsenates from wastewaters on blast furnace dust slurry was discussed by Carrillo-Pedroza et al. [7] – the adsorption mechanism was characterized by Langmuir adsorption isotherm and the dominant retention mechanism was the formation of Fe^{2+} and Fe^{3+} arsenates as corrosive products. Adsorption of phosphate anions from aqueous solutions is studied namely for slag materials. Other solid metallurgical wastes are used for this purpose rather scarcely. For example, crystalline (BFSC) and amorphous (BFSAS) blast furnace slags were used for phosphate removal [8]. Disintegrated slag (BFS-D) was tested as an adsorbent of phosphate from aqueous solutions by Kostura et al. [9]. An excellent linear relationship between the retention capacities and optical basicities of model BFSAS was observed [10]. Granulated blast furnace slag (BFGS) was used for the retention of phosphates from wastewaters by Korkusuz et al. [11]. In all these cases, precipitation of Ca phosphates was concluded as the dominant retention mechanism. The removal of phosphates from solutions by steel-making slag (SMS) and magnetic separation was studied by Xiong et al. [12]. In the case of blast-furnace dust slurry (BFSd), it was concluded that the adsorption of phosphates from the solution was given by Freundlich isotherm and reached its maximum at pH 5–7 [13].

This study deals with the evaluation of the retention mechanisms of phosphate anions from aqueous solutions on steel-making and convertor dust slurry. The attention is paid also to the effect of acidic leaching on retention characteristics of the aforementioned dust slurry samples and the possibility of desorption of retained phosphates.

2. EXPERIMENTAL

Prepration of dust slurry samples. For the adsorption of phosphates from aqueous solutions two types of metallurgical wastes – steel-making dust slurry (SS) and convertor dust slurry (CS) – were tested along with their solid residues after acidic leaching

(SSL and CSL, respectively). Both original dust slurry samples were collected in the Northern Moravian industrial agglomeration. The samples were ground and sieved to prepare a particle size of <0.1 mm. SSL and CSL samples were prepared by leaching 40 g of SS/CS in 1000 cm^3 of 1 M HCl for 24 h followed by filtration, rinsing by distilled water (once), and drying at 105 °C.

Sample characterization. Determination of elemental concentrations in the studied samples was carried out employing X-ray fluorescence spectrometry using homogenized samples with a particle size <50 μm. Fusion machine VULCAN 4MA was used for the preparation of 40-mm fusion beads using lithium tetraborate as a flux. The XRF analysis itself was conducted using wavelength-dispersive X-ray fluorescence spectrometer ARL PERFORM'X (Switzerland) equipped with 4200 W X-ray tube (with 50-μ Be window), 2 detectors (FPC, SC), 9 crystals, 4 primary collimators, and elemental mapping function. All analyses were conducted under a vacuum.

The specific surface area of samples was measured at 77 K under vacuum (<1 Pa) using Sorptomatic 1990 device (ThermoFinnigan, Italy) with gaseous nitrogen as adsorbate. The specific surface areas were calculated according to the Brunauer–Emmet –Teller (BET) theory in the range of relative pressures of 0.05–0.25. The sizes of micro- and mesopores were evaluated using the Horwath–Kawazoe, and Barrett–Joyner –Halenda models, respectively.

Determination of phase composition of the studied samples was conducted by X-ray diffraction analysis using a fully automated URD-6 diffractometer (Rich Seifert-FPM, Germany) operating at radiation CoK_{α}, 40 kV, 35 mA. The obtained data were digitalized using the RayfleX Software (RayfleX ScanX a RayfleX Analyze, version 2.289). Phosphate (as phosphorus) was determined spectrophotometrically as phosphomolybdenum blue on a UV spectrophotometer (UV-1800 Shimadzu, Japan).

The IR spectra of all samples were measured by the potassium bromide pellets technique. Exactly 1.0 mg of the sample was ground with 200 mg dried potassium bromide. This mixture was used to prepare the potassium bromide pellets. The pellets were pressed by 8 t for 30 s under vacuum. The infrared spectra were collected using FTIR spectrometer Nicolet iS50 (Thermo Scientific, USA) with DTGS detector. Following parameters were used for measurement: spectral region 4000–400 cm^{-1}, spectral resolution 4 cm^{-1}, 64 scans, Happ–Genzel apodization. Treatment of spectra: polynomial (second order) baseline, subtraction spectrum of pure potassium bromide.

Raman spectra of all samples were measured using a 180-deg measurement technique without any sample preparation. Raman spectra were recorded at dispersive Raman spectrometer DXR SmartRaman (Thermo Scientific, USA) with CCD detector. The measurement parameters were as follows: excitation laser 780 nm, grating 400 lines/mm, aperture 50 μm, exposure time 1 s, number of exposures 250, and the spectral region 2000–50 cm^{-1}. An empty sample compartment was used for background measurement. Treatment of spectra: fluorescence correction (6th order).

Adsorption kinetics. To evaluate the adsorption kinetics, a series of suspensions containing 0.5 g of adsorbent and 100 cm^3 of phosphate solution (500 mg PO_4^{3-}/dm^3) were prepared. Suspensions were agitated in a horizontal shaking apparatus at 180 r/min and after a given dwell time (1, 3, 8, 24, 72 or 120 h) they were filtered. Prepared filtrates were used for the spectrophotometric evaluation of residual phosphate (as phosphorus). Experimentally determined data were evaluated by kinetic model for pseudo-second order reaction:

$$\frac{dQ_t}{dt} = k\left(Q_{P,\max} - Q_t\right)^2 \tag{1}$$

where $Q_{P,\max}$, and Q_t, mg/g, are amounts of phosphate (as phosphorus) adsorbed in equilibrium and at time t, respectively, k is the equilibrium rate constant of pseudo-second order sorption, g/(mg·h).

Isotherm models. For phosphates uptake from water solutions on SS and CS samples, batch experiments at room temperature were performed. 100 cm^3 aqueous solutions containing different P concentrations and 0.5 g of dust slurry were applied. Aqueous solutions (10–500 mg PO_4^{3-}/dm^3) were prepared from KH_2PO_4 salt. Suspensions were agitated in a horizontal shaking apparatus vibrated at the rate of 180 min^{-1} for 5 days and then filtered.

The equilibrium data determined for the uptake of PO_4^{3-} (as P) on SS, CS, SSL, and CSL samples were fitted with the Langmuir, Modified Langmuir, and Freundlich isotherms. The corresponding relationships for these models are given by Eqs. (2)–(4).

The Langmuir isotherm (A):

$$Q_P = \frac{Q_{P,\max} k_1 c_P}{1 + k_1 c_P} \tag{2}$$

where Q_P, mg/g, is the quantity of PO_4^{3-} (as P) adsorbed on SS and CS samples, c_P is the equilibrium concentration of the solute, mg/dm^3, $Q_{P,\max}$ represents the maximum sorbate uptake, mg/g, and k_1 is the coefficient relating to the affinity between the solute and the sorbent, dm^3/mg.

The Modified Langmuir isotherm (B):

$$\frac{Q_P}{Q_{P,\max}} = \frac{K c_P^x}{1 + K c_P^x} \tag{3}$$

where $Q_{P,\max}$, mg/g, is the maximum quantity of PO_4^{3-} (as P) adsorbed on SS and CS samples, K, $(dm^3/mg)^x$, is the affinity constant for adsorption and x is a constant characterizing the heterogeneity of the system.

The Freundlich isotherm (C):

$$Q_P = k_F c_P^{1/n} \tag{4}$$

where k_F, (mg/g)/(mg/dm^3)$^{1/n}$, and n are the Freundlich constants related to the adsorption quantity and intensity respectively.

Desorption tests. For the determination of the phosphate desorption scale, 100 cm^3 of desorption agent (5% aqueous solutions of $AlCl_3$ or Na_2CO_3) was added to the filter cake (0.5 g of dust slurry). Dust slurry samples saturated with phosphates were designated SS_{sat}, CS_{sat}, and CSL_{sat}. These suspensions were agitated in a horizontal shaking apparatus that vibrated at the rate of 180 min^{-1} during 24 h, and then filtered. The whole process was repeated once more.

3. RESULTS AND DISCUSSION

3.1. TEXTURAL CHARACTERISTICS

Specific surface areas of both original dust slurry samples determined by S^{BET} method are given in Table 1 along with their other textural characteristics.

Table 1

Textural characteristics of original SS and CS and their leached analogs

Sample	Density [g/cm^3]	Specific surface area [m^2/g]	Mesopore volume [cm^3/g]	Micropore volume [cm^3/g]
SS	4.96	7.77	0.047	0.002
CS	5.08	4.19	0.024	0.001
SSL	5.03	7.30	0.043	0.002
CSL	5.01	12.72	0.018	0.003

Data summarized in Table 1 indicate that the sludges SS and CS and their leached analogs (SSL and CSL) are non-porous materials of comparable density whose specific surface areas are usually below 10 m^2/g.

3.2. CHEMICAL COMPOSITION

The chemical composition of original and leached dust slurry samples is summarized in Table 2. Contents of mineral phases in original and leached dust slurry samples are listed in Table 3. The data in Table 3 indicate that both original dust slurry samples differ in the level of the amorphous phase. In CS, the level of the amorphous phase is dominant and reaches 80 wt. %. In leached samples, it is nearly the same as in original

slurry samples before their acidic leaching. The percentages of dissolved mass during the leaching for SS and CS samples were 27.7 and 65 wt. %, respectively.

Table 2

Chemical composition [wt. %] of original (SS and CS) and leached (SSL and CSL) samples

Oxide	Sample			
	SS	SSL	CS	CSL
SiO_2	1.62	1.24	2.48	2.96
TiO_2	0.019	0.02	0.076	0.05
Al_2O_3	0.15	0.11	0.31	0.96
Fe_{total}	56,02	58.76	58.85	72.73
MnO	1.21	1.21	1.14	0.61
CaO	0.99	0.25	7.82	0.24
MgO	0.68	0.52	2.40	0.28
ZnO	10.27	7.97	0.70	0.11
Na_2O	–	–	0.22	0.30
K_2O	0.12	0.07	0.06	0.06
C	1.51	1.60	4.31	12.40
SO_3	0.24	0.09	0.35	0.485
P_2O_5	0.21	0.18	0.23	0.18

Table 3

Contents of mineral phases in original (SS and CS) and leached (SSL and CSL) samples

Mineral	Sample			
	SS	SSL	CS	CSL
Amorphous phase	42.70	44.80	80.61	85.74
Magnetite	34.67	34.62	1.94	3.94
Wüstite	2.68	2.80	7.22	4.56
Hematite	–	–	1.01	1.28
Zincite	1.42	0.02	–	–
Franklinite	15.62	14.62	–	–
Iron α	–	–	0.84	0.96
Merwinite	–	–	3.09	2.09
Calcite	–	–	1.68	–
Periclase	–	–	1.37	–
Portlandite	–	–	1.46	–
Grafite	2.88	3.13	0.78	1.43

Both dust slurry samples contain Fe associated with oxidic minerals. In SS and SSL samples, the dominant occurrence of Fe is related to Fe_3O_4; much less abundant are

franklinite and wüstite. In the original dust slurry, Zn occurs in two forms: predominantly as franklinite ($ZnFe_2O_4$) which is hardly soluble in acids, and less abundantly as zincite (ZnO) which is an easily soluble form.

In CS and CSL, the most abundant oxidic form of Fe is wüstite (FeO) which prevails over magnetite (Fe_3O_4). CS contains also a noticeable level of Ca- and Mg-bearing minerals (calcite, merwinite, periclase, portlandite). Leached sample CSL does not contain these phases (with the only exception of merwinite) as they were dissolved during acidic leaching.

3.3. KINETIC MEASUREMENTS

Experimental data for the retention of phosphate over time for both original dust slurry samples is depicted in Fig. 1. The experimental data in Fig. 1 indicate that the sorption equilibrium became nearly reached after ca. one day and it was fully established after 5 days. Evaluation of the experimental data according to Eq. (1) revealed that the sorption of phosphates on both types of dust slurry samples could be described by pseudo-second order kinetic model. Calculated values of kinetic parameters are summarized in Table 4.

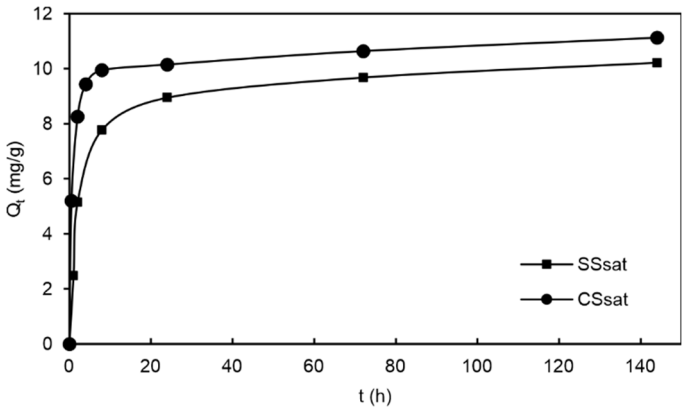

Fig. 1. Dynamic adsorption of phosphate on dust slurry samples SS_{sat} and CS_{sat}; 0.5 g of adsorbent, 100 cm^3 of phosphate solution, 500 mg PO_4^{3-}/dm^3

Table 4

Calculated constants of pseudo-second order kinetics

Sample	R^2	k [g/(mg·h)]	$Q_{P,\max}$ [mg/g]
SS	0.9995	$5.73 \cdot 10^{-4}$	10.34
CS	0.9995	$1.38 \cdot 10^{-3}$	11.11

3.4. ADSORPTION TESTS

The results and the calculated values of corresponding constants for individual isotherm models are shown in Table 5. The data suggest that the sorption of phosphates on the studied dust slurry samples can be described by both Langmuir (or modified Langmuir) or Freundlich adsorption isotherms. The observation is in agreement with the conclusion of other researchers studying the adsorption of phosphates on similar oxidic materials. For example, the sorption of phosphates on blast furnace slags can be characterized by Langmuir isotherm [8]. In the case of slags from oxygen converters, the experimental data can be fitted by Langmuir and Freundlich isotherm models (Freundlich isotherm model was slightly better) [14]. To describe the sorption on iron oxide tailings, the Langmuir–Freundlich isotherm was used [15]. The aforementioned results indicate that the retention of phosphates from aqueous solutions on the studied wastes is a complex combination of chemical and physical processes.

Table 5

Calculated constants for the isotherm models

Sample	Calculated values	Model						
		Langmuir		Modified Langmuir			Freundlich	
		$Q_{P,\max}$ [mg/g]	k_1 [dm^3/mg]	x	$Q_{P,\max}$	K [(dm^3/mg)^x]	k_F [(mg/g)/ (mg/dm^3)$^{1/n}$]	n
SS	Constants	10.93	0.029	1.0	10.93	0.029	0.481	1.517
	R^2	0.979		0.979			0.933	
CS		10.99	0.169	1.2	10.93	0.118	5.335	7.369
	R^2	0.957		0.961			0.923	
CSL		11.43	0.127	1.2	11.30	0.084	5.118	7.148
	R^2	0.942		0.952			0.906	

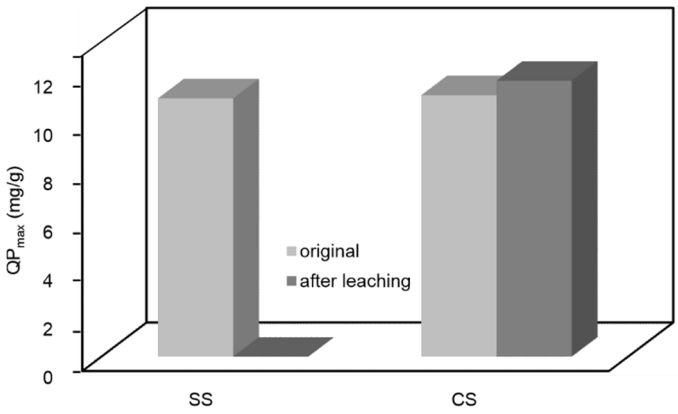

Fig. 2. The Langmuir retention capacities
of original dust slurry samples and samples after acidic leaching

Adsorption experiments revealed comparable sorption ability of the original dust slurry samples (Fig. 2). In contrast, leached dust slurry samples exhibited significantly different sorption efficiencies – SSL sample nearly did not sorbed phosphates at all, whereas CSL sample retained phosphates with the same efficiency as an original non-leached sample. Maximum saturation capacities calculated from the Langmuir isotherm were: for SS slurry 10.93 mg P/g, for CS it was 10.99 mg P/g and for CSL it was 11.43 mg P/g.

These calculated values of the maximum saturation capacities expressed as mg P/g are comparable with those of blast furnace slags and are higher than saturation capacities observed by other authors on similar materials and by-products from metallurgical processes (Table 6). These materials and by-products from metallurgical processes are blast furnace dust slurry (BFSd) [11], crystalline blast furnace slag (BFSC) [8], amorphous blast furnace slag (BFSAS) [8], granulated blast furnace slag (BFSG) [11], steel-making slag (SMS) [12] and convertor slag (CVS) [16].

Table 6

Sorption capacities ($Q_{P,\max}$) for the slag samples and other alternative adsorbents

Adsorbent	BFSd	BFSC	BFSAS	BFSG	SMS	CVS
$Q_{P,\max}$, mg/g	2.87	13.42	6.47-8.50	9.15	5.30	2.14

3.5. IR AND RAMAN SPECTROSCOPIC ANALYSIS

For the determination of the nature of retained phosphates, IR spectra of original metallurgical wastes and the samples saturated with phosphates were measured. In CS and CSL samples, Raman spectra as well to further specification and interpretation IR spectra were used. The results for sample SS are depicted in Fig. 3.

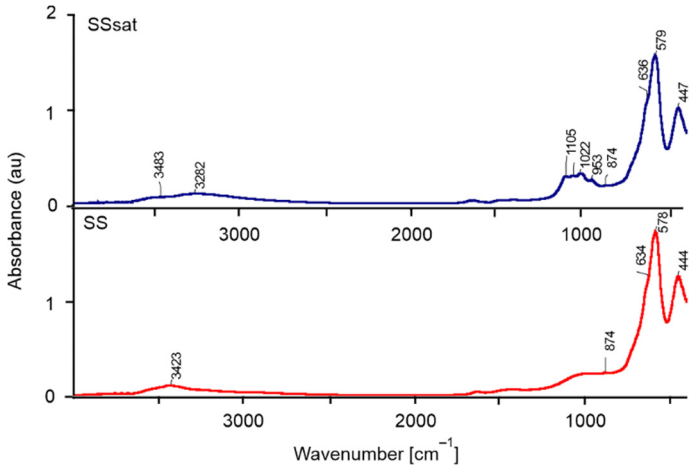

Fig. 3. IR spectra of an original sample before (SS) and after (SS_{sat}) phosphate adsorption

IR spectrum of the dust slurry saturated with phosphates (SS_{sat}) provides new bands in the range of 1200–900 cm^{-1}. The bands at 1061cm^{-1} and 1105 cm^{-1} can be attributed to asymmetric and symmetric vibrations of P–O bond in phosphate group PO_4^{3-}, respectively. The band at 953 cm^{-1} could be assigned to P–O–Zn vibrations [17, 18]. Hence, the surface complexes of phosphates and zincite are probably formed, for instance, following the equation [18].

$$ZnO\ (s) + H_2O + HPO_4^{2-} \rightarrow Zn(OH)_2HPO_4^{2-} \quad (5)$$

As zincite was dissolved during acidic leaching, SSL practically lost its ability to retain phosphates.

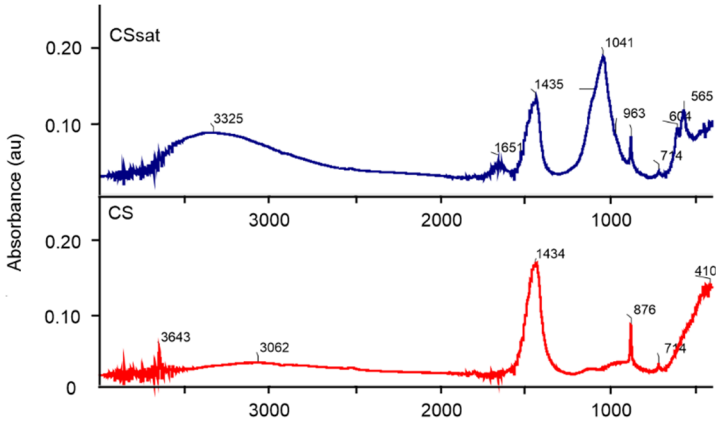

Fig. 4. IR spectra of original convertor dust slurry (CS) before and after (CS_{sat}) phosphate adsorption

IR spectra of original convertor dust slurry (CS) before and after (CS_{sat}) phosphate adsorption are shown in Fig. 4. In the spectra of CS_{sat}, there are overlapped bands in the range of 1200–900 cm^{-1} with dominant at 1037 cm^{-1}, which belong to asymmetric vibrations P–O–P in the phosphate group. As this band is not present in the spectrum of CS sample, it corresponds with the phosphate retained from the solution – probably Ca-phosphate [19] or some form of Fe-phosphates [20]. The band at ca. 600 cm^{-1} in the CS_{sat} spectrum indicates the presence of $FePO_4 \cdot 2H_2O$ [21]. Very broad bands at ca. 3350 cm^{-1} and a band at 1655 cm^{-1} are due to the presence of water in the sample CS_{sat}. Various forms of water should be taken into account, also crystalline water which could indicate the formation of Fe-phosphate dihydrate. Strong bands at 1434 cm^{-1}, narrow bands at 875 cm^{-1}, and weak bands at ca. 720 cm^{-1} in the spectrum of the dust slurry before and after phosphate sorption are attributed to carbonate anions. With the view of higher calcium content in CS sample (Table 2), the occurrence of calcite $CaCO_3$ can be expected. Further

specification of retained phosphates can be achieved by examination of the Raman spectra of CS samples before and after the uptake of phosphates (Fig. 5).

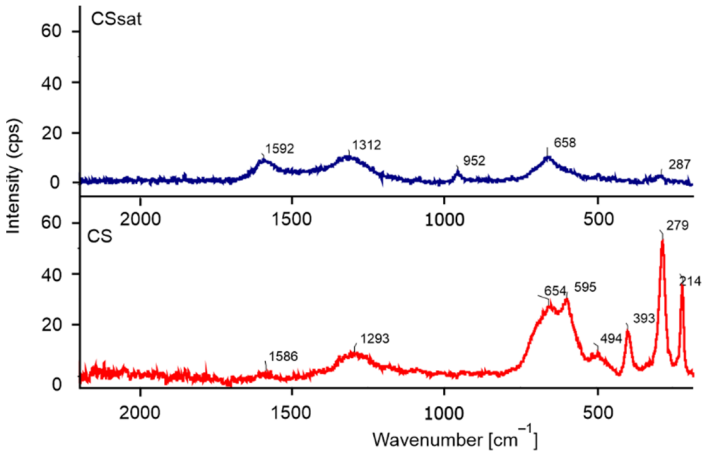

Fig. 5. Raman spectra of original dust slurry
before (CS) and after (CS_{sat}) phosphate adsorption

In Figure 5, significant differences are visible between the spectra of CS and CS_{sat} samples in the range of 750–200 cm^{-1}. Strong bands in the spectrum of CS are typical of hematite [22]. They disappear in CS_{sat} spectrum, pointing to Fe(III)–PO_4 interaction. A very weak band at 952 cm^{-1} in the spectrum of CS_{sat} can be assigned to P–O vibration in phosphates [21]. Two bands in the range of 1700–1200 cm^{-1} present in the spectra of both samples could be attributed to D and G bands of graphite.

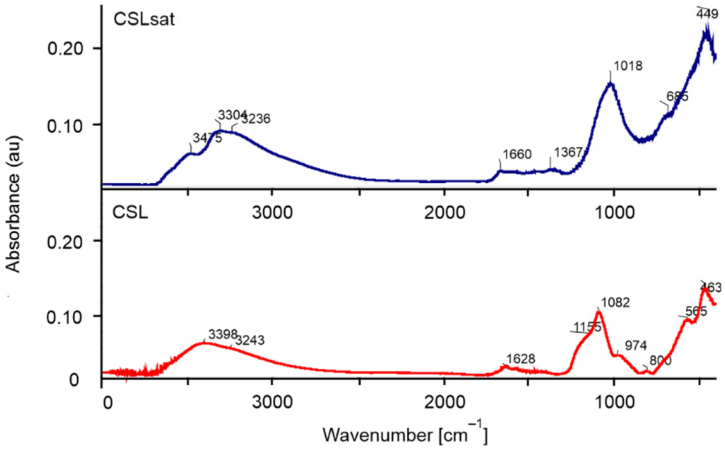

Fig. 6. IR spectra of residues after acidic leaching
before (CSL) after phosphate adsorption (CSL_{sat})

IR spectra of the CSL sample before and after its saturation with phosphates (CSL_{sat}) are shown in Fig. 6. After acidic leaching, the bands at 1434 and 875 cm^{-1} disappeared; these bands are attributed to the vibration of the carbonate group in calcite $CaCO_3$. The bands at the range of 3500–3000 and 1700–1600 cm^{-1} in the spectra of both samples confirm the presence of various forms of water. The differences are visible again in the lower wavenumber region. In the spectrum of CSL sample, the bands within the region of 1200–800 cm^{-1} are due to silicates, the bands at 566 and 462 cm^{-1} originate from Fe-oxides, respectively [23]. In the spectrum of CSL_{sat}, the bands assigned to silicates in the region of 1200–800 cm^{-1} contain a strong and broad band at 1013 cm^{-1}, which is attributed to the phosphate group in Fe-phosphates. It might be related to the formation of $FePO_4 \cdot 2H_2O$ or the formation of surface protonated and non-protonated monomolecular and bimolecular Fe-phosphate complexes, as shown in [24]. The formation of these surface complexes can be expected at pH < 7.5 [25]:

$$\text{surface-Fe–OH} + HPO_4^{2-} \rightarrow \text{surface-Fe–}PO_4^{2-} + H_2O \quad (6)$$

$$\text{surface-Fe–}PO_4^{2-} + H^+ \rightarrow \text{surface-Fe–}PO_4H^- \quad (7)$$

$$\text{surface-Fe–}PO_4H^- + H^+ \rightarrow \text{surface-Fe–}PO_4H_2 \quad (8)$$

The equilibrium pH of phosphate leachates after sorption was around 6.5. Raman spectra of CSL and CSL_{sat} are shown in Fig. 7.

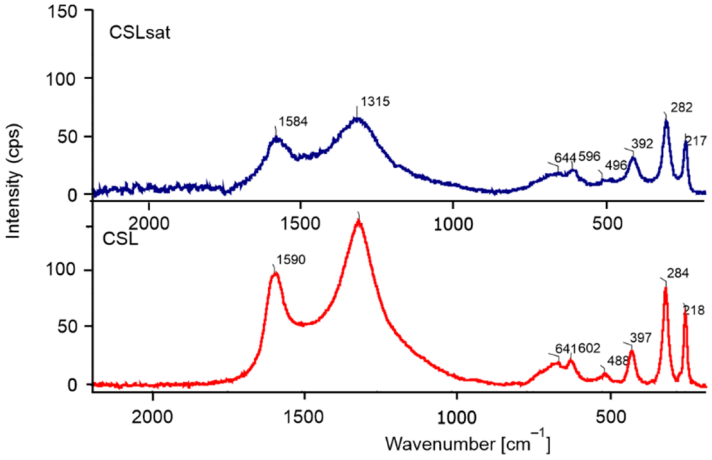

Fig. 7. Raman spectra of residues after acidic leaching before (CSL) and after phosphate adsorption (CSL_{sat})

The differences between these two spectra occur in the lower wavenumber region of 750–200 cm^{-1}. From the doublet at 605 and 649 cm^{-1} (in the spectrum of CSL), the band at 605 cm^{-1} (in the spectrum of CSL_{sat}) disappears again. Other hematite bands are

significantly less intensive, pointing to partial interaction of Fe(III)-PO_4. The spectrum of CSL_{sat} contains a very weak band of P–O vibration of phosptates at 940 cm^{-1} [21].

From the comparison of mineral crystalline phases of CS dust slurry before and after acidic leaching (CSL) presented in Table 3, it is evident that acidic leaching preferentially removed easily soluble calcium and magnesium phases from the dust slurry whereas Fe-oxides remain in the residue after leaching. Iron bound in oxides facilitates the retention of phosphate anions and leads to surface co-precipitation or complexation of Fe-phosphates.

Analysis of IR and Raman spectra showed that the retention of phosphates by SS and CS samples was based on different mechanisms even though their sorption capacities are comparable. This is consistent with the fact that acidic leaching significantly changed the sorption characteristics of both dust slurry samples.

3.6. RESULTS OF DESORPTION TESTS

SS_{sat}, CS_{sat}, and CSL_{sat} samples were used for desorption tests. Obtained results are summarized in Table 7, from which it can be deduced that the best desorption agent for all the studied samples is $AlCl_3$. In contrast, poor desorption of phosphates was observed if water was used as a desorption agent.

Table 7

Desorbed phosphates (as P, wt. %) previously sorbed by samples SS_{sat}, CS_{sat} and CSL_{sat}

Sample	Desorption agent		
	$AlCl_3$ solution (5 wt. %)	H_2O	Na_2CO_3 solution (5 wt. %)
SS	85.35	10.39	69.42
CS	96.66	12.14	72.55
CSL	100	2.82	78.39

4. CONCLUSIONS

Both original dust slurry samples exhibited similar sorption capacities that are comparable with blast-furnace slags. The equilibrium was established after 6 days and the sorption process can be characterized by the Langmuir and Freundlich isotherm models which indicates the occurrence of the physical and chemical processes. Nevertheless, the retention mechanisms are different for both dust slurry samples. In steel-making dust slurry, the retention is based on the formation of surface complexes with zincite. The high solubility of zincite phase in acidic solution is the predominant reason for suppressed sorption of phosphates on the leached dust slurry. In non-leached convertor dust

slurry, the formation of Ca and Fe phosphates is very likely; after leaching, the formation of surface protonated and non-protonated mono- and bimolecular Fe-complexes is probable as well. Despite rather different retention mechanisms, both dust slurry samples exhibited similar desorption behavior. The most efficient release of phosphates from all studied samples was observed in weakly acidic solutions whereas in water the phosphates desorption was very low. The achieved results can be used for the treatment of municipal/industrial wastewater.

ACKNOWLEDGEMENTS

This paper was created within the frame of the project number SP2020/44 financed by the Ministry of Education, Youth and Sports of the Czech Republic and the project number CZ.02.1.01/0.0/0.0/17_049/0008426 financed by the Operational Programme Research, Development and Education under the auspices of the Ministry of Education, Youth and Sports of the Czech Republic.

REFERENCES

[1] BUSÉ R., MOMBELLI D., MAPELLI C., *Metals recovery from furnaces dust. Waelz process*, Metall. Ital., 2014, 106 (5), 19–27. DOI: hdl.handle.net/11311/924357.

[2] ZHANG D., ZHANG X., YANG T., RAO S., HU W., LIU W., CHEN L., *Selective leaching of zinc from blast furnace dust with mono-ligand and mixed-ligand complex leaching systems*, Hydrometall., 2017, 169, 219–228. DOI: j.hydromet.2017.02.003.

[3] LOÂ PEZ-DELGADO A., PEÂ REZ C., LOÂ PEZ F.A., *Sorption of heavy metals on blast furnace sludge*, Water Res., 1998, 32, 989–996. DOI: 10.1016/S0043-1354(97)00304-7.

[4] RADJENOVIC A., MALINA J., STRKALJ A., *Removal of Ni from aqueous solution by blast furnace sludge as an adsorbent*, Desalin. Water Treat., 2010, 21, 286–294. DOI: 10.5004/dwt.2010.1580.

[5] ROZUMOVÁ L., PREHRADNÁ J., *Reducing the content of metal ions from mine water by using converter sludge*, Water, 2018, 10 (1), 38. DOI: 10.3390/w10010038.

[6] KLIKA Z., SEIDLEROVÁ J., VALÁŠKOVÁ M., KLIKOVÁ C., KOLOMAZNÍK I., *Uptake of Ce(III) and Ce(IV) on montmorillonite*, Appl. Clay Sci., 2016, 132–133, 41–49. DOI: 10.1016/j.clay.2016.05.012.

[7] CARRILLO-PEDROZA F.R., DE JESÚS SORIA-AGUILAR M., MARTÍNEZ-LUEVANOS A., NARVAEZ-GARCÍA V., *Blast furnace residues for arsenic removal from mining-contaminated groundwater*, Environ. Technol., 2014, 2895–2902. DOI: 10.1080/09593330.2014.925509.

[8] KOSTURA B., KULVEITOVÁ H., LEŠKO J., *Blast furnace slags as sorbents of phosphate from water solutions*, Water Res., 2005, 39, 1795–1802. DOI: 10.1016/j.watres.2005.03.010.

[9] KOSTURA B., DVORSKÝ R., KUKUTSCHOVÁ J., ŠTUDENTOVÁ S., BEDNÁŘ J., MANČÍK P., *Preparation of sorbent with a high active sorption surface based on blast furnace slag for phosphate removal from wastewater*, Environ. Prot. Eng., 2017, 43, 161–168. DOI:10.5277/epe170113.

[10] KOSTURA B., HUCZALA R., RITZ M., LEŠKO J., *Retention of phosphates from aqueous solutions within sol-gel derived amorphous $CaO–MgO–Al_2O_3–SiO_2$ system as a model of blast furnace slag*, Chem. Pap., 2018, 72 (2), 401–408. DOI: 10.1007/s11696-017-0289-2.

[11] KORKUSUZ E.A., BEKLIOĞLU M., DEMIRER G.N., *Use of blast furnace granulated slag as a substrate in vertical flow reed beds. Field application*, Bioresour. Technol., 2007, 98, 2089–2101. DOI: 10.1016/j.biortech.2006.08.027.

[12] XIONG J.B., HE Z.L., MAHMOOD Q., LIU D., YANG X., ISLAM E., *Phosphate removal from solution using steel slag through magnetic separation*, J. Hazard. Mater., 2008, 152, 211–215. DOI: 10.1016/j.jhazmat.2007.06.103.

[13] KOSTURA B., KULVEITOVÁ H., LEŠKO J., *Determination of phosphorus forms after sorption on blast furnace sludge and slag*, Hutnické listy, 2002, 6–8, 7–12 (in Czech).

[14] XUE Y., HOU H., ZHU S., *Characteristics and mechanisms of phosphate adsorption onto basic oxygen furnace slag*, J. Hazard. Mater., 2009, 162, 973–980. DOI: 10.1016/j.jhazmat.2008.05.131.

[15] ZENG L., LI X., LIU J., *Adsorptive removal of phosphate from aqueous solutions using iron oxide tailings*, Water Res., 2004, 38, 1318–1326. DOI: 10.1016/j.watres.2003.12.009.

[16] YANG J., WANG S., LU Z.B., YANG J., LOU S.J., *Converter slag-coal cinder columns for the removal of phosphorous and other pollutants*, J. Hazard. Mater., 2009, 168, 331–337. DOI: 10.1016/j.jhazmat.2009.02.024.

[17] BIAO W., YUPEN Y., YUANZHI T., YUGE B., FAN L., WENFENG T., QIAOYUN H., XIONGHAN F., *Effects of polyphosphates and orthophosphate on the dissolution and transformation of ZnO nanoparticles*, Chemosphere, 2017, 176, 255–265. DOI: 10.1016/j.chemosphere.2017.02.134.

[18] MICHELMORE A., JENKINS P., RALSTON J., *The interaction of linear polyphosphates with zincite surfaces*, Int. J. Miner. Process., 2003, 68, 1–16. DOI: 10.1016/S0301-7516 (01)00085-0.

[19] MAITZ M.F., PHAM M.T., MATZ W., REUTHER H., STEINER G., *Promoted calcium-phosphate precipitation from solution on titanium for improved biocompatibility by ion implantation*, Surf. Coat. Techn., 2002, 158–159, 151–156. DOI: 10.1016/S0257-8972 (02)00189-5.

[20] KHAN I., SUNAKAWA K., HIGASHINAKA R., MATSUDA T.D., AOKI Y., NOMURA K., KUZMANN E., HOMONNAY Z., SINKÓ K., NAKA T., NAKANE T., KREHULA S., MUSUĆ S., KUBUKI S., *Structural characterization and magnetic properties of iron-phosphate glass prepared by sol-gel method*, J. Non-Cryst. Solids, 2020, 543, 120158. DOI: 10.1016/j.jnoncrysol.2020.120158.

[21] ZAGHIB K., JULIEN C.M., *Structure and electrochemistry of $FePO_4 \cdot 2H_2O$ hydrate*, J. Power Sources, 2005, 142, 279–284. DOI: 10.1016/j.jpowsour.2004.09.042.

[22] JUBB A.M., ALLEN H.C., *Vibrational spectroscopic characterization of hematite, maghemite, and magnetite thin films produced by vapor deposition*, ACS Appl. Mater. Interf., 2010, 2, 2804–2812. DOI: 10.1021/am1004943.

[23] RUAN H.D., FROST R.L., KLOPROGGE J.T., *The behavior of hydroxyl units of synthetic goethite and its dehydroxylated product hematite*, Spectrochim. Acta Part A, 2001, 57, 2575–2586. DOI: 10.1016/S1386-1425 (01)00445-0.

[24] ARAI Y., SPARKS D.L., *ATR-FTIR spectroscopic investigation on phosphate adsorption mechanisms at the ferrihydrite–water interface*, J. Colloid Interface Sci., 2001, 241, 317–326. DOI: 10.1006/jcis.2001.7773.

[25] HUANG X., *Intersection of isotherms for phosphate adsorption on hematite*, J. Colloid Interface Sci., 2004, 271, 296–307. DOI: 10.1016/j.jcis.2003.12.007.